

Optimization planning of energy storage based on multi-objective improved particle swarm and droop control algorithm

Yujie Qin

Northwest Minzu University, Lanzhou 730030, China

Abstract: Based on the nonlinear loads of distributed power sources, large-scale deployment can easily lead to problems such as overvoltage, reverse power flow, and harmonic circulation. In this paper, we constructed a multi-objective optimization planning model for distributed energy storage in active distribution networks using an improved particle swarm optimization algorithm and an improved droop control algorithm. A splitting strategy was introduced in the improved particle swarm algorithm to increase population diversity and reduce the number of local optima. The optimization planning model was built with the minimum sum of voltage vulnerability multi-indicators as the main objective. Furthermore, to better eliminate harmonic circulation in the power grid system under the impact of a large amount of nonlinear loads, this paper also designed and improved the LCL filter at the output of the inverter and reintroduced a new droop quantity in the traditional droop control. Adjusting the two links proportionally, the effectiveness and applicability of the proposed distributed energy storage optimization planning method were verified through simulation examples.

Keywords: Distributed Energy Storage, Improved Particle Swarm Algorithm, Splitting Strategy, Improved Droop Control Algorithm

1. Introduction

The "14th Five-Year Plan" for renewable energy development points out that renewable energy will gradually become the main force to support economic and social development. New energy represented by wind power and photovoltaic power is showing a trend of rapidly improving performance, sustained economic benefits, and accelerating application scale expansion^[1]. Distributed generation (DG) is a new product of renewable energy development, but it is difficult to be widely deployed due to issues such as overvoltage and harmonic circulation^[2-3]. The development of energy storage technology has brought new solutions to DG, namely Distributed Energy Storage (DES), which can alleviate network congestion, reduce peak-valley difference, reduce network losses, and act as an emergency power source in case of faults^[4]. However, if DES is not appropriately configured in the distribution network, with its characteristics of being numerous and scattered, it may increase the volatility and randomness of the power grid. Therefore, it is of great practical significance to establish an optimization model that takes into account both safety and economic efficiency^[5-6].

Wang Jinan et al.^[7] proposed a prediction power model and balanced optimization control strategy that accurately tracks dynamic currents and effectively improves the load balance of DG. Liu Wenxia et al.^[8] proposed an energy storage optimization scheme for distribution systems, which provides useful theoretical support for improving energy storage investment benefits. Sun Jian et al.^[9] proposed a fault recovery strategy for priority islanding and used whale algorithm to restructure non-fault areas to restore power supply. Fang Lei et al.^[10] used an improved NSAG-III optimization algorithm and proposed the offset crossover operation method for positional variables. Wang Lina^[11] used an improved particle swarm optimization algorithm, significantly improving the comprehensive benefits of the energy storage system and reducing the waste of photovoltaic power.

In this paper, an improved particle swarm algorithm will be used for multi-objective optimization of the energy quality indicators of DES. A new droop quantity will be reintroduced in the traditional droop control to improve and optimize its topology and control strategy, increase the system's ability to carry loads, and reduce system losses.

2. Analysis of Power Grid Vulnerability and Nonlinear Load Indicators

2.1 Quantitative Treatment of Voltage Quality

This paper intends to start from the perspective of node voltage quality. If this indicator is larger, it means that the voltage at the current node is more unstable, the power supply energy quality is lower, and the system's ability to resist risks is lower, and vice versa [12]. At any moment, the vulnerability index of node i in the power grid can be represented as:

$$\eta(t) = \left| \frac{v_t - v_0}{0.07v_0} \right| \quad (1)$$

In the equation, v_t represents the voltage size of node i at time t , and v_0 is the rated voltage of node i . Since DG is generally distributed at the user end and the power grid is connected at 35kV or below, the allowable deviation of the power supply voltage is $\pm 7\%$ of the rated voltage.

2.2 Quantitative Treatment of System Power Losses

In the power grid system, the charging and discharging process of DES can be equivalent to loads and power sources, that is, absorbing or releasing power from the distribution system. In this paper, the circuit parameters of each branch node in the power grid are taken as optimization factors for solving [13].

$$\sigma = \sum_{i,j=0}^{\kappa} \frac{(V_i - V_j)^2 + 2V_i V_j (1 - \cos \varphi_{ij})}{R_{ij}} \quad (2)$$

In the equation, V_i and V_j represent the voltages of nodes i and j , respectively, φ_{ij} is the phase angle difference between nodes i and j , R_{ij} is the total input resistance between nodes i and j , and κ is the set of all nodes in the system.

2.3 Planning of LCL Filter Inductance and Capacitance

In a filtering circuit, the lower limit of inductance is generally determined by the current ripple in the circuit, with an upper limit value of 20% selected in this paper.

In actual parallel systems, power factor should not be too low, so the requirement for capacitance is to control its absorption of reactive power to be less than 5%. The reactive power of the circuit can be expressed as [14]:

$$Q_c = 3\omega \cdot C \cdot V^2 \quad (3)$$

3. Development of the Improved Algorithm

3.1 Improved Multi-Objective Particle Swarm Optimization Algorithm

The optimization process of Particle Swarm Optimization usually selects global and local optimals based on the evaluation results, that is, fitness values. The global optimal represents the position with the highest fitness value for all particles up to now [14], which is represented as:

$$F_{gb} = \min \{ F_{pb1}, F_{pb2}, \dots, F_{pbend} \} \quad (4)$$

And is updated iteratively according to the following formula:

$$\begin{cases} F_j(a+1) = F_j(a) + F_j(a+1) \\ v_j(a+1) = wv_j(a) + c_1r_1(F_{pb}(a) - F_j(a)) + c_2r_2(F_{gb}(a) - F_j(a)) \end{cases} \quad (5)$$

In the formula, F_{gb} represents the global best position, F_{pb} represents the local best position, j

represents the particle number, a represents the current iteration number, c_1 is the individual learning factor used to control the step size of particles moving towards the local best direction, and c_2 is the global learning factor used to control the step size of particles moving towards the global best direction.

In addition, the improved algorithm used in this paper also introduces a splitting strategy. During the iteration process, the clustered particles are adaptively segmented and leapfrogged to avoid local optimization problems. The splitting condition is as follows:

$$\begin{cases} \frac{F_j}{F_{j,gb}} < Z \\ Z = Z_0 \left(1 - \frac{k}{k_{\max}}\right) \end{cases} \quad (6)$$

By constraining the above condition, the splitting strategy for each particle is given as follows:

$$g_j(k) = \frac{a}{a_{\max}} g_j(a) + D \left(1 - \frac{a}{a_{\max}}\right) g_j(a) \quad (7)$$

Where $g_j(k)$ represents the position of particle i after k iterations, and D is the dynamic splitting operator.

The flowchart of the improved algorithm is shown in Figure 1:

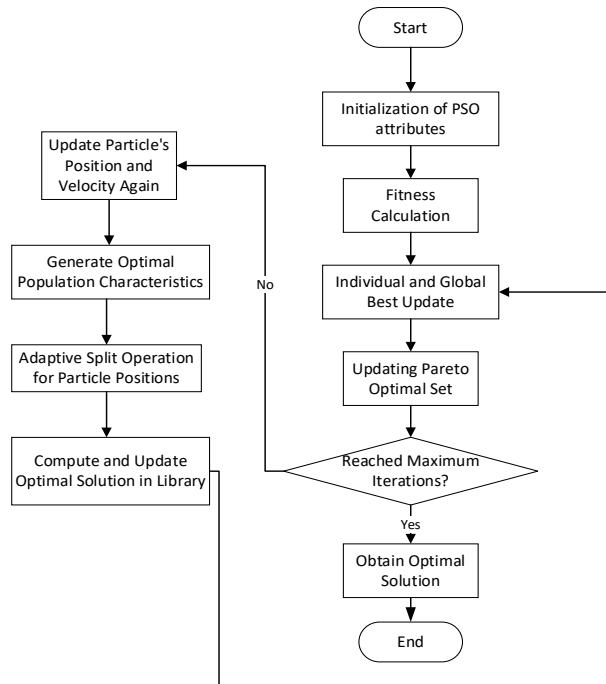


Figure 1: Flowchart of improved particle swarm optimization algorithm

3.2 Improved droop control algorithm

Let $A = R/Z$ and $B = X/Z$ quantify the influence of the presence of resistive and inductive on the frequency and amplitude of the output voltage. The expression of the improved droop control is as follows:

$$\begin{cases} \omega_i = \omega_i^* - mB(P_i - P_i^*) + nA(Q_i - Q_i^*) \\ U_i = U_i^* - m_1A(P_i - P_i^*) + n_1B(Q_i - Q_i^*) \end{cases} \quad (8)$$

Where m, n, m_1, n_1 are droop coefficients of active and reactive power for the frequency and amplitude of the output voltage. When the impedance between power systems has pure resistance characteristics, the parallel output power is expressed as follows:

$$\begin{cases} P_i = \frac{U_i U_i \phi_i}{Z_i} \\ Q_i = \frac{U_i (U_i - U_L)}{Z_i} \end{cases} \quad (9)$$

Taking the example of inverter parallel connection, assuming a hypothetical potential of the output end of the inverter parallel connection, it is assumed that Inverter $\phi_1 > \phi_2$ in the parallel connection, in this state, the frequency increase of the second inverter in parallel is obviously greater than that of the first inverter, namely Inverter $\Delta f_1 > \Delta f_2$. Assuming that after adjusting one cycle, Inverter $\Delta f_1 = \Delta f_2$ is in this state, and Inverter $\Delta f = \Delta f_1 - \Delta f_2$. At the same time, the phase angle of the output voltage of the first inverter is reduced by $\Delta\phi = \Delta\phi_1 - \Delta\phi_2$ compared with the phase angle of the output voltage of the second inverter, and according to the above assumptions, it can be concluded that:

$$\Delta f = n(Q_1 - Q_2) = \Delta f_1 - \Delta f_2 = \frac{(\phi_1 - \phi_2)}{2\pi T} = \frac{(Q_2 - Q_1)R}{2\pi T U_L^2} \quad (10)$$

The equivalent model diagram of inverter parallel connection is shown in Figure 2:

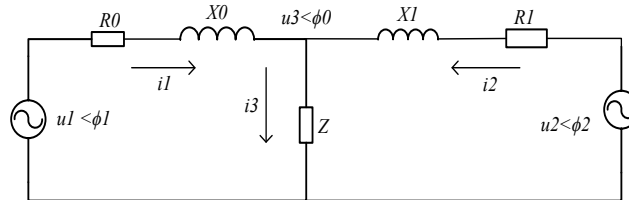


Figure 2: Shows the equivalent model of an inverter parallel connection system

From this equation, the droop coefficient can be obtained as follows:

$$n = \frac{-R}{2\pi T U_L^2} \quad (11)$$

4. Simulation analysis

4.1 IEEE-33 Simulation Analysis

This article establishes a simulation example based on the data of the IEEE-33 node system^[12]. Nodes 11 and 32 are connected to distributed wind turbines, and nodes 16 and 21 are connected to distributed photovoltaics for simulation analysis. The IEEE-33 node diagram is shown in Figure 3:

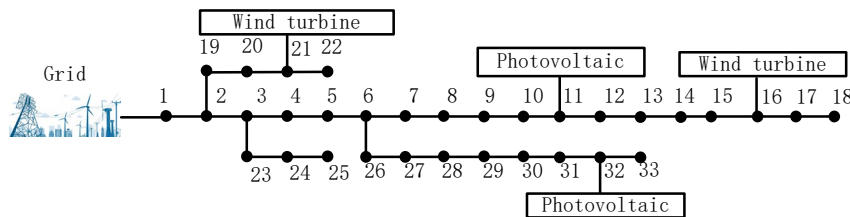


Figure 3: IEEE-33 Circuit Diagram

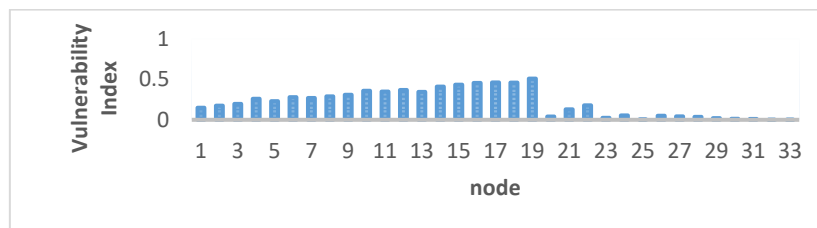


Figure 4: Vulnerability Index of Voltage at 21:00

We selected the time with the most severe voltage deviation at 21:00 at night as the reference time and analyzed the voltage vulnerability indicators of each node.

From Figure 4, it can be seen that the nodes with high voltage vulnerability indicators are mostly terminal nodes in the radial network.

The comparison of the load curves before and after energy storage configuration is shown in Figure 5.

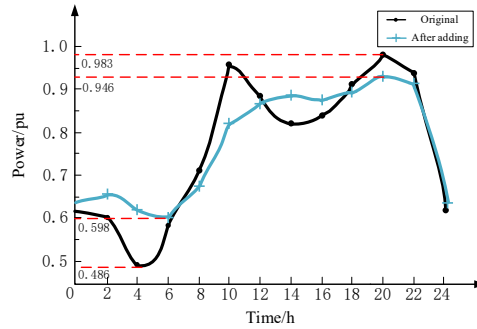


Figure 5: Comparison of System Load Curves

From Figure 5, it can be seen that the optimized energy storage operation strategy has a certain peak-shaving effect, which has a positive effect on improving the utilization and safety of generation equipment.

4.2 Simulation analysis of LCL filtering circuit

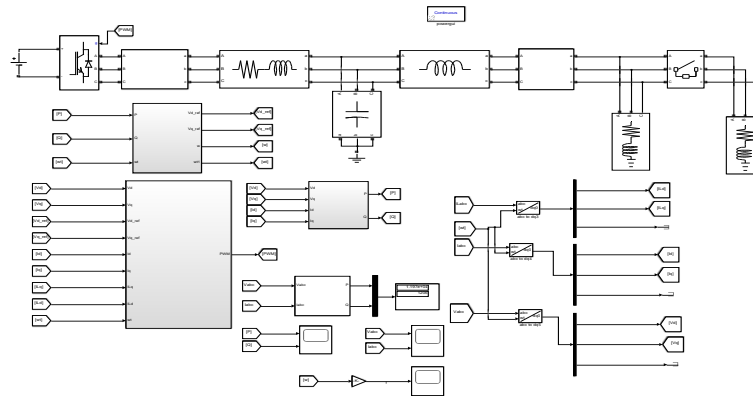


Figure 6: Droop Control Model

In order to better verify the practicality and scientificity of the proposed optimization strategy, a model of droop control system for LCL filtering circuit was built on the SIMULINK simulation platform. The droop control model is shown in Figure 6.

4.3 Simulation Results

The simulation system diagram from Figure 7 to Figure 10 shows that the design improvement of the LCL circuit and the improvement of the droop control can better solve the problem of harmonic circulating current. It can also provide certain protection for the impact and harm caused by the appearance of nonlinear elements under fault conditions in the system.

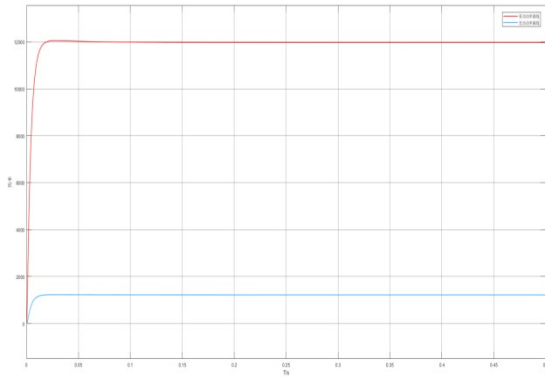


Figure 7: Reactive and Active Power Curve

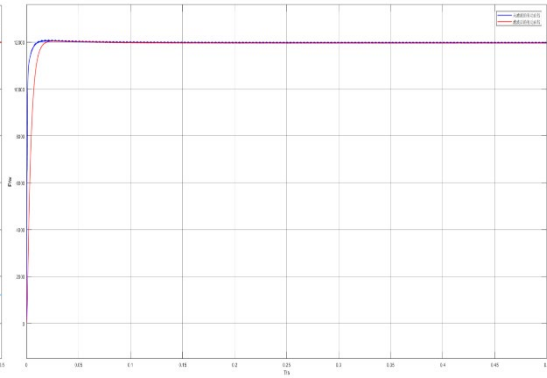


Figure 8: Compare power with/without filtering

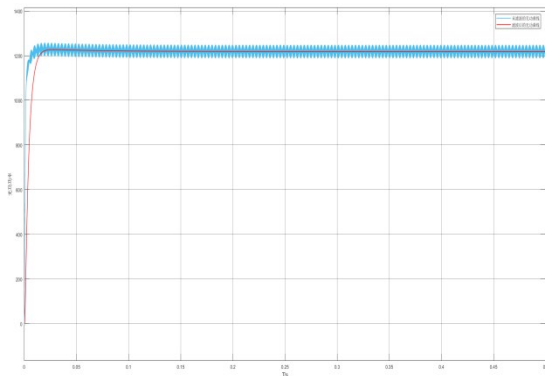


Figure 9: Filtering effect on reactive power curve

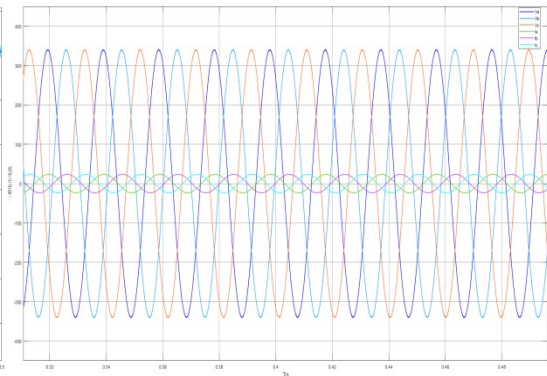


Figure 10: Curve after increasing reactive power

5. Summary

The simulation results of the case study show that: 1) Improved droop control algorithm: in a system with droop control and LCL filtering, the system's reactive and active power output curves will be smoother and more stable around the load. The waveforms of the active and reactive power after filtering are smoother. After sudden non-linear load, the output active power, reactive power and frequency of the system, under the dual mechanism of LCL filtering and droop control, may increase within a certain range, but will be controlled within the permissible range, suppressing harmonic circulating currents and making the system more stable; 2) Improved particle swarm optimization algorithm: Compared with the original algorithm, the improved algorithm has stronger global optimization ability, which can effectively reduce the vulnerability and losses of the active power grid, improve the operational safety and economic efficiency of active distribution networks, and maintain the voltage level of each node in the system within a reasonable range after energy storage is connected.

References

- [1] Li X. Nine departments including the National Development and Reform Commission issued "Renewable Energy Development Plan for the 14th Five-Year Plan Period" [J]. *Equipment engineering in China*, 2022, No. 501(13): 1.
- [2] Zhao D, Xu C, Tao R, et al. A comprehensive review of the flexible regulation of multi-type distributed energy storage systems on the distribution side of the new power system. *Proceedings of the Chinese Society for Electrical Engineering*, 2023, 43(05): 1776-1799. DOI: 10.13334/j.0258-8013.pcsee.220778.
- [3] Bhatti M Z A, Siddique A, Aslam W, et al. Improved Model Predictive Direct Power Control for Parallel Distributed Generation in Grid-Tied Microgrids [J]. *Energies*, 2023, 16(3): 1441.
- [4] Silva C, Faria P, Fernandes A, et al. Clustering distributed Energy Storage units for the aggregation of optimized local solar energy [J]. *Energy Reports*, 2022, 8: 405-410.
- [5] Zhang Y, Zhang S, Liu S, Yi Y, et al. Double-Layer Planning of Distribution Transformers with Distributed Photovoltaics and Energy Storage Integration [J]. *Power System Protection and Control*, 2020, 48(24): 9-15. DOI: 10.19783/j.cnki.pspc.200128.

- [6] Adewumi O B, Fotis G, Vita V, et al. *The impact of distributed energy storage on distribution and transmission networks' power quality* [J]. *Applied Sciences*, 2022, 12(13): 6466.
- [7] Wang J, Xu J, et al. *Optimization Control Strategy for Battery State of Charge Balancing in Distributed Energy Storage Type MMCs* [J/OL]. *Electric Power Automation Equipment: 1-9* [2023-03-13].
- [8] Liu W, Yang M, Wang J, et al. *Optimized Configuration of Energy Storage in Incremental Distribution Systems Based on Intelligent Generation of Operational Strategies* [J]. *Journal of Chinese Electrical Engineering*, 2021, 41(10): 3317-3329+3658. DOI: 10.13334/j.0258-8013.pcsee.200655.
- [9] Sun J, Yu Z, et al. *Self-Healing Strategy for Distribution Networks with Distributed Energy Storage Systems Considering Load Demand Response* [J/OL]. *Journal of Wuhan University of Technology (Engineering Edition): 1-15* [2023-03-13].
- [10] Fang L, Xue Y, Chi Y, et al. *Multi-Objective Siting and Sizing Method for Distributed Energy Storage Systems with Integrated Operation Planning* [J]. *Smart Grid*, 2022, 50(11): 1-8.
- [11] Wang L. *Research on Optimal Configuration of Energy Storage System Based on Improved Particle Swarm Optimization Algorithm* [D]. *China University of Mining and Technology*, 2021. DOI: 10.27623/d.cnki.gzkyu.2021.001616.
- [12] Mu J. *Multi-Objective Optimization of Distributed Energy Storage in Active Distribution Networks* [D]. *Shaanxi University of Technology*, 2022. DOI: 10.27733/d.cnki.gsxlq.2022.000280.
- [13] Deng S. *Optimal Planning of Distributed Energy Storage in Distribution Networks under Multiple Uncertainties* [D]. *North China Electric Power University (Beijing)*, 2022. DOI: 10.27140/d.cnki.ghbbu.2022.000875.
- [14] Wang Y, Ma C, Wang C, et al. *Characteristics analysis and optimization design of bridge crane based on improved particle swarm optimization algorithm* [J]. *Journal of Low Frequency Noise, Vibration and Active Control*, 2023, 42(1): 253-271.